



# Copper increases reductive dehalogenation of haloacetamides by zero-valent iron in drinking water: Reduction efficiency and integrated toxicity risk



Wenhai Chu<sup>a,\*</sup>, Xin Li<sup>a</sup>, Tom Bond<sup>b</sup>, Naiyun Gao<sup>a</sup>, Xu Bin<sup>a</sup>, Qiongfang Wang<sup>a</sup>, Shunke Ding<sup>a</sup>

<sup>a</sup> State Key Laboratory of Pollution Control and Resources Reuse, Institute of Disinfection By-product Control in Water Treatment, College of Environmental Science and Engineering, Tongji University, Shanghai, 200092, China

<sup>b</sup> Department of Civil and Environmental Engineering, Imperial College London, London, SW7 2AZ, UK

## ARTICLE INFO

### Article history:

Received 21 June 2016

Received in revised form

16 October 2016

Accepted 19 October 2016

Available online 19 October 2016

### Keywords:

Disinfection byproducts

Haloacetamides

Dechlorination

Zero-valent iron/copper

Integrated toxicity risk

Drinking water

## ABSTRACT

The haloacetamides (HAcAms), an emerging class of nitrogen-containing disinfection byproducts (N-DBPs), are highly cytotoxic and genotoxic, and typically occur in treated drinking waters at low  $\mu\text{g/L}$  concentrations. Since many drinking distribution and storage systems contain unlined cast iron and copper pipes, reactions of HAcAms with zero-valent iron (ZVI) and metallic copper (Cu) may play a role in determining their fate. Moreover, ZVI and/or Cu are potentially effective HAcAm treatment technologies in drinking water supply and storage systems. This study reports that ZVI alone reduces trichloroacetamide (TCaAm) to sequentially form dichloroacetamide (DCAm) and then monochloroacetamide (MCAm), whereas Cu alone does not impact HAcAm concentrations. The addition of Cu to ZVI significantly improved the removal of HAcAms, relative to ZVI alone. TCAm and their reduction products (DCAm and MCAm) were all decreased to below detection limits at a molar ratio of ZVI/Cu of 1:1 after 24 h reaction (ZVI/TCaAm = 0.18 M/5.30  $\mu\text{M}$ ). TCAm reduction increased with the decreasing pH from 8.0 to 5.0, but values from an integrated toxic risk assessment were minimised at pH 7.0, due to limited removal MCAm under weak acid conditions (pH = 5.0 and 6.0). Higher temperatures (40 °C) promoted the reductive dehalogenation of HAcAms. Bromine was preferentially removed over chlorine, thus brominated HAcAms were more easily reduced than chlorinated HAcAms by ZVI/Cu. Although tribromoacetamide was more easily reduced than TCAm during ZVI/Cu reduction, treatment of tribromoacetamide resulted in a higher integrated toxicity risk than TCAm, due to the formation of monobromoacetamide (MBAcAm).

© 2016 Elsevier Ltd. All rights reserved.

## 1. Introduction

Nitrogenous disinfection by-products (N-DBPs) have received increasing attention because they are more toxic than the regulated trihalomethanes (THMs) and haloacetic acids (HAAs) (Plewa et al., 2007, 2008; Yang and Zhang, 2013; Liu and Zhang, 2014; Chu et al., 2015a). As a result of rapid population growth and rising water demand, drinking water source waters are facing threats of insufficiently treated wastewater discharges and algal blooms (Shah and

Mitch, 2012; Chu et al., 2015b). These polluted water sources are characterized by higher levels of dissolved organic nitrogen (Dotson and Westerhoff, 2009; Liu et al., 2013), which is linked to their frequent occurrence in chlor(am)inated drinking water (Krasner et al., 2006, 2013; Richardson et al., 2008, Richardson and Ternes, 2014; Goslan et al., 2009; Bond et al., 2011, 2015; Chu et al., 2012; Hou et al., 2012). Among these N-DBPs, haloacetamides (HAcAms) were found to be highly cytotoxic and genotoxic in mammalian cell assays, i.e.  $142 \times$  more cytotoxic and  $12 \times$  more genotoxic than HAAs (Plewa et al., 2007; Richardson et al., 2007). They are the most cytotoxic of all DBP classes measured to-date, and are the second-most genotoxic DBP class, just behind the halonitriles (Plewa and Wanger, 2015; Richardson and Postigo, 2015). Among HAcAms, dichloroacetamide (DCAm) is typically

\* Corresponding author. College of Environmental Science and Engineering, Tongji University, Room 308 Mingjing Building, 1239 Siping Road, Yangpu District, Shanghai, 200092, China.

E-mail addresses: [feedwater@126.com](mailto:feedwater@126.com), [1world1water@tongji.edu.cn](mailto:1world1water@tongji.edu.cn) (W. Chu).

found at the highest concentration, with trichloroacetamide (TCaAm) and monochloroacetamide (MCAAm) reported infrequently in low-bromide sources (Krasner et al., 2006; Richardson et al., 2007; Chu et al., 2012). The elevated toxicity of TCAAm and DCAAm were also observed in the recent studies based on metabonomics (Zhang et al., 2013; Yu et al., 2015), and DCAAm presented significantly higher cytotoxicity and genotoxicity than halomethanes (Yang et al., 2014). While chlorinated HACams tend to occur at higher concentrations than their brominated analogues in drinking water (Krasner et al., 2006; Bond et al., 2011; Chu et al., 2012), the latter are actually more cytotoxic and genotoxic (Plewa et al., 2008). Therefore, it is important to control both chlorinated and brominated HACams in drinking water.

Generally, DBP control strategies can be divided into three categories: (1) removal of DBP precursors prior to disinfection, (2) modification of disinfection practices to minimize DBP formation, and (3) removal of DBPs after formation. It has been reported that various pre-treatments in drinking water treatment plants (DWTPs) can achieve good removal of HACAm precursors (Chu et al., 2011, 2014, 2015a; Xie et al., 2013), as well as for other N-DBPs (Bond et al., 2011; Shah et al., 2012). Efforts have also been made to study HACAm formation mechanisms with the purpose of acquiring the knowledge to reduce their formation during chlorination (Shah and Mitch, 2012; Huang et al., 2012; Wang et al., 2014; Chu et al., 2015b). However, DBP formation can also occur in water distribution systems, due to reactions involving residual chlorine (Rossman et al., 2001). There remains an information gap on the removal of N-DBPs after their formation.

The polar nature of HACams (Fig. SM1), including MCAAm, DCAAm and TCAAm, suggests that reductive dehalogenation is a potential route for their removal. Furthermore, the end products of dehalogenation (i.e. non-chlorinated acetamide) are of low-toxicity to humans and the environment (Plewa et al., 2008). This motivated us to consider the potential of reductive dehalogenation technologies to reduce the levels of HACams in drinking water.

Since Gillham and O'Hannesin discovered that metallic iron fillings could be utilized in groundwater remediation (Gillham and O'Hannesin, 1994), the use of zero-valent iron (ZVI, Fe<sup>0</sup>) for in-situ remediation of groundwater contaminated by chlorinated organic compounds has received considerable attention (Dries et al., 2004; He et al., 2010; Kohn et al., 2005; Liu and Lowry, 2006; Zhang et al., 2011). Moreover, to enhance dehalogenation and prolong the activity of ZVI, a second transition metal (e.g. Pd, Ni, Ru and Pt) with high hydrogenation ability can be incorporated in a bimetal system, such as applied for the remediation of carbon tetrachloride (Feng and Lim, 2007; Wang et al., 2009), chloroform (Feng and Lim, 2007; Wang et al., 2009), dichloromethane (Feng and Lim, 2007; Wang et al., 2009), tetrachloroethylene (Lien and Zhang, 2001; Zhang et al., 1998), trichloroethylene (Lien and Zhang, 2001; Tee et al., 2009; Zhang et al., 1998), dichloroethene (Lien and Zhang, 2001; Zhang et al., 1998), 1,1-dichloroethane (Cwierny et al., 2006), 1,1,1-trichloroethane (Cwierny et al., 2006; Lien and Zhang, 2001), and 1,1,2,2-tetrachloroethane (Lien and Zhang, 2005).

Finished drinking water is often distributed from DWTPs to consumers by unlined cast iron pipes, and sometimes copper pipes (Ridgway et al., 1981; McNeill and Edwards, 2001; Lin et al., 2001; Niquette et al., 2000). During distribution, drinking water is also often stored in storage ponds made from iron materials, with copper materials also sometimes used to inhibit the growth of microorganisms (Kooij et al., 2005; Teng et al., 2008; Critchley et al., 2001; Lehtola et al., 2004). It is important to proactively examine the potential of ZVI, Cu, and their combination (ZVI/Cu) for the reductive dehalogenation of HACams and possible application in drinking water distribution and storage systems. Therefore, the objective of this study was to examine the potential of three

reductive dehalogenation technologies - ZVI alone, Cu alone, and combined ZVI/Cu - for removing HACams in drinking water. This is the first study to report findings about N-DBP removal by reductive dehalogenation methods. Both chlorinated and brominated HACams were considered. The changes of HACams concentrations and integrated toxic risk caused by HACams were also examined.

## 2. Materials and methods

### 2.1. Materials

MCAAm (98.5%), DCAAm (98.5%) and TCAAm (99%) standards were obtained from Alfa Aesar (Karlsruhe, Germany), and five bromine-containing HACams (bromochloroacetamide [BCAAm], dibromoacetamide [DBAAm], bromodichloroacetamide [BDCAAm], dibromochloroacetamide [DBCACAm] and tribromoacetamide [TBACAm]) were purchased from Orchid Cellmark (New Westminster, BC, Canada). Monobromoacetamide (MBAAm) and three HAAs (monochloroacetic acid [MCAA], dichloroacetic acid [DCAA] and trichloroacetic acid [TCAA]) were supplied by Sigma-Aldrich (St Louis, Missouri, USA). Sodium acetate anhydrous, 2-(N-morpholino)ethanesulfonic acid (MES, 99%) and tris(hydroxymethyl)aminomethane (TRIS, 99.9%) were purchased from Aladdin Industrial Inc (Shanghai, China). The ZVI ( $\geq 99.99\%$ ) and copper ( $\geq 99.99\%$ ) powders were also supplied by Sigma-Aldrich (St Louis, Missouri, USA). Ultrapure water was produced with a Millipore Milli-Q Gradient water purification system (Billerica, MA, USA). All the other chemical reagents were at least of analytical grade, and obtained from Sinopharm Chemical Reagent Co., Ltd (Shanghai, China) unless otherwise noted.

### 2.2. Experimental procedure

Batch reduction tests were performed by adding selected doses of ZVI and/or Cu powder (doses range: ZVI = 0.2–10.0 g/L [0.004–0.179 M]; ZVI/Cu molar ratio = 1:1, except as noted) to 250-mL sealed glass bottles containing 50 mL one of the following trihalogenated HACams: TCAAm, BDCAAm, DBCACAm or TBACAm (5.30  $\mu\text{M}$ , except as noted). Before each experiment the reaction bottles were purged with nitrogen to remove air. Each run lasted for 24 h and the bottles were placed on a water bath shaker at 150 r/m to make the solid and liquid well-mixed and keep the temperature constant at  $25 \pm 0.2$  °C unless otherwise noted. Sodium acetate (0.1 M), MES (0.03 M) and Tris (0.05 M) were used as a pH  $7.0 \pm 0.2$  buffer (Keenan and Sedlak, 2008) unless otherwise noted.

### 2.3. Analytical methods

At selected time intervals, 10 mL of reaction solution was filtered through 0.22  $\mu\text{m}$  syringe filters and 4 g anhydrous sodium sulfate was added into the filtered sample. Then HACams were immediately extracted into 2 mL methyl tert-butyl ether (MTBE), and were analyzed using gas chromatography (GC) coupled with an electron capture detector (ECD) (QP 2010 plus, Shimadzu, Japan). Injections of 1.0  $\mu\text{L}$  of the extract were introduced via a splitless injector onto a GC column (RTX-5, 30-m  $\times$  0.25-mm ID, 0.25- $\mu\text{m}$  film thickness). The column oven was initially held at 40 °C for 10 min, ramping to 200 °C at 20 °C/min and holding for 2 min. The injection port was controlled at 180 °C and the ECD detector temperature was 320 °C. Three HAAs (MCAA, DCAA and TCAA) were also analyzed by the GC/ECD (QP 2010 plus, Shimadzu, Japan) according to US EPA method 552.2 (USEPA, 1995; Chu et al., 2014). The detection limits for TCAAm, DCAAm, MCAAm, TCAA, DCAA, and MCAA were 0.01, 0.01, 0.05, 0.05, 0.05, and 0.07  $\mu\text{M}$ , respectively. Brominated HACams, were analyzed by combining high pressure liquid

chromatography and triple-quadrupole mass spectrometry (HPLC/tqMS). The HPLC (e2695) from Waters (Milford, MA), employing a Hypersil GOLD C18 packed column (100 × 2.1 mm i.d., 5 μm) with a Hypersil GOLD precolumn (10 × 2.1 mm i.d., 5 μm) (Thermo Scientific; Waltham, MA) was used for separation. After separation, a tqMS (TSQ Quantum Access MAX) from Thermo Scientific (Waltham, MA) was used to detect all brominated HACams by positive atmospheric pressure chemical ionization combined with the selective reaction monitoring mode. The optimal operating parameters were as follows: discharge current at 4.0 μA, vaporizer temperature at 350 °C, sheath gas pressure at 40 psi, capillary temperature at 250 °C, and collision pressure at 1.5 m Torr. Detection limits for all brominated HACam were below 0.01 μM. More details of the DBP analyses are presented elsewhere (Krasner et al., 2006; Chu et al., 2012, 2014). All samples were prepared in triplicate and the error bars in the figures represent the standard deviations from triplicate measurements. Relative standard deviations (n = 3) of all samples were all below 7%.

### 3. Results and discussion

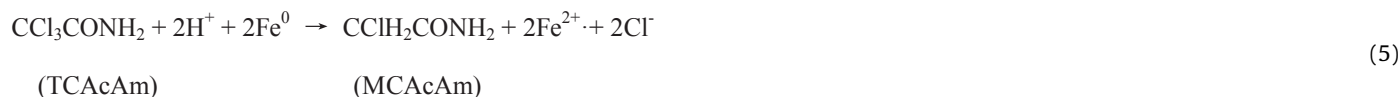
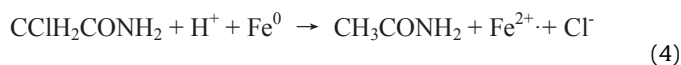
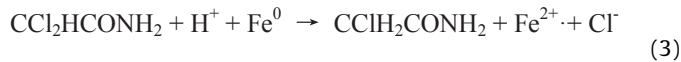
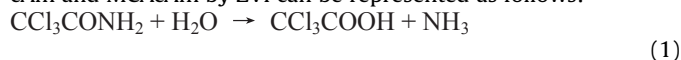
#### 3.1. Reduction of chlorinated HACams by ZVI

Fig. 1 shows the time-dependent changes of concentrations for three chlorinated HACams (TCaAm, DCAcAm and MCAcAm) at different ZVI doses. As shown in Fig. 1a, at a low ZVI dose (0.2 g/L), TCAcAm concentrations slightly decreased from the initial  $5.30 \pm 0.27 \mu\text{M}$  to  $4.57 \pm 0.23 \mu\text{M}$  over 24 h, which equates to a very low pseudo-first-order reduction rate of  $0.01 \text{ h}^{-1}$  (Table SM1). In contrast, at higher ZVI doses (5.0 g/L and 10.0 g/L), TCAcAm concentrations presented a significant reduction and the pseudo-first-order reduction rate increased to  $0.18 \text{ h}^{-1}$  and  $0.43 \text{ h}^{-1}$ , respectively (Table SM1). After 24 h, TCAcAm was completely removed at ZVI doses of 5.0 g/L and 10.0 g/L.

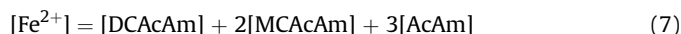
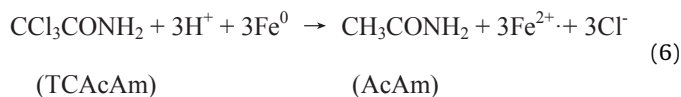
As shown in Fig. 1b and c, DCAcAm and MCAcAm were both undetectable after 24 h at the lowest ZVI dose (0.2 g/L). This indicated the slight reduction of TCAcAm at the low ZVI dose (0.2 g/L) was probably due to the very slow hydrolysis of TCAcAm at pH 7.0 (Glezer et al., 1999; Reckhow et al., 2001; Chu et al., 2009a), as shown in Equation (1), rather than dechlorination. It should be noted that the hydrolysis of TCAcAm, DCAcAm and MCAcAm is all

the higher doses (Wang and Zhang, 1997; Xia et al., 2014).

Many environmentally significant contaminants, such as the chlorinated hydrocarbons mentioned above, can serve as the ultimate electron acceptors during reductive dehalogenation. Likewise, the reduction of HACams by different iron species is essentially a surface-mediated, electrocatalytic reaction. Generally, the possible dehalogenation pathways for these contaminants can be divided into three categories: (i) direct electron transfer from ZVI to chlorinated hydrocarbons; (ii) reduction by ferrous iron ( $\text{Fe}^{2+}$ ) formed from ZVI reduction; and (iii) electrocatalytic reduction by hydrogen formed from ZVI reduction (Guan et al., 2015). We examined the impact of  $\text{Fe}^{2+}$  by dosing  $\text{Fe}^{2+}$  instead of ZVI under the same reaction conditions, and found TCAcAm concentrations did not significantly change, and DCAcAm and MCAcAm were not detected over 24 h (Fig. SM2). Most researchers accept that the reductive dechlorination of chlorinated organics occurs on the surface of ZVI by pathway (i) (Equations (2)–(6)), because the reduction rate of chlorinated organics by pathways (ii) and (iii) is very slow (House, 1972; Warren et al., 1995; Maithreepala and Doong, 2004). Based on dechlorination pathway (i) (direct electron transfer from iron to chlorinated hydrocarbons), the dechlorination of TCAcAm, DCAcAm and MCAcAm by ZVI can be represented as follows:



negligible in 24 h when solution pH is lower than 7.0 (Chu et al., 2009a, 2013). This was also been confirmed by our control experiments. When the ZVI dose increased to 5.0 g/L, DCAcAm concentrations increased from initial value of  $<0.01 \mu\text{M}$  to  $1.64 \pm 0.08 \mu\text{M}$  and  $1.67 \pm 0.08 \mu\text{M}$  after 6 h and 12 h respectively, before decreasing to  $0.92 \pm 0.05 \mu\text{M}$  at 24 h (Fig. 1b). Data at 10.0 g/L followed a similar pattern, except no DCAcAm was detected after 24 h. Furthermore, MCAcAm increased over a 24 h period, from an initial value below the detection limit to  $0.47 \mu\text{M}$  (ZVI dose = 5.0 g L<sup>-1</sup>). At a higher dose of ZVI (10 g L<sup>-1</sup>), MCAcAm first increased to  $0.58 \pm 0.03 \mu\text{M}$  after 12 h and then decreased to  $0.26 \pm 0.01 \mu\text{M}$  by 24 h (Fig. 1c). As shown in Fig. 1d, the sum of three HACam concentrations also decreased as the ZVI dose increased from 0.2 g/L to 10.0 g/L. The enhancement in the reduction of three HACams with increasing ZVI dosages was probably due to the increasing availability of adsorption/reduction sites at



As shown by Equation (2), reduction of 1 M TCAcAm to DCAcAm will produce 1 M  $\text{Fe}^{2+}$ . As shown in Equation (5), generated by merging Equations (2) and (3), if 1 M TCAcAm is reduced to MCAcAm, 2 M  $\text{Fe}^{2+}$  will be formed. Similarly, if 1 M TCAcAm was reduced to acetamide (AcAm), 3 M  $\text{Fe}^{2+}$  will be formed (Equation (6), generated by merging Equations (2) (3) and (4)). Therefore, the

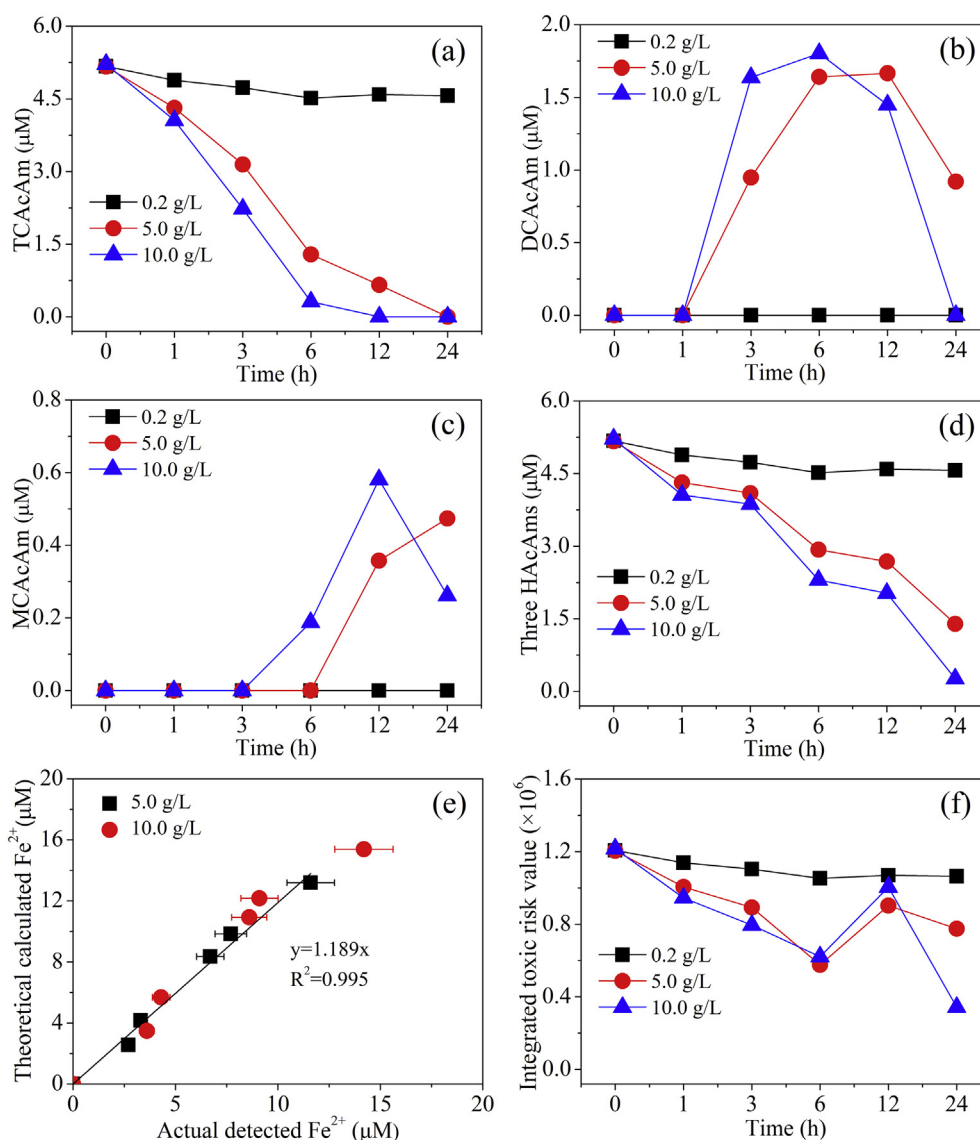


**Fig. 1.** Influence of ZVI dosage on the removal of HACAs. (Initial TCaAm molar concentration = 5.30  $\mu\text{M}$  [DCAcAm and MCAcAm were not added]; **a**, TCaAm; **b**, DCAcAm; **c**, MCAcAm; **d**, total HACaMs [sum of three HACaM concentrations]; **e**, comparison of the theoretical calculated  $\text{Fe}^{2+}$  concentrations and the actual detected  $\text{Fe}^{2+}$  concentrations; **f**, integrated toxic risk caused by HACaMs at different ZVI dosages.)

$\text{Fe}^{2+}$  formed by dechlorination of TCaAm with ZVI should theoretically equal the sum of [DCAcAm], twice the [MCAcAm] and three times [AcAm] (AcAm concentration is equal to the initial TCaAm minus the remaining TCaAm as well as the formation of DCAcAm and MCAcAm), with concentrations in moles (Equation (7)). As shown in Fig. 1e, there is a good correlation between the theoretical  $\text{Fe}^{2+}$  concentrations calculated using the equations above and the actual detected  $\text{Fe}^{2+}$  concentrations from 1 h to 24 h at pH 7.0. Further, the actual detected  $\text{Fe}^{2+}$  concentrations were slightly lower than the theoretical calculated  $\text{Fe}^{2+}$  (the slope is 1.19), indicating limited Fe oxide was formed on ZVI, because the reaction was conducted under anaerobic conditions. Overall, the strong correlation between the theoretical calculated  $\text{Fe}^{2+}$  concentrations and the actual detected  $\text{Fe}^{2+}$  concentrations (Fig. 1e) and the formation of DCAcAm (Fig. 1b) and MCAcAm (Fig. 1c) suggest direct dechlorination of TCaAm by ZVI was the primary operative reaction process, in agreement with the recent study discovering the direct reduction of Se (IV) by detecting  $\text{Fe}^{2+}$  release

(Liang et al., 2014).

### 3.2. Integrated toxic risk caused by HACaMs during ZVI dehalogenation

Plewa and colleagues systematically investigated the cytotoxicity and genotoxicity of HACaMs (Plewa et al., 2008), and found the combined toxicity values (cytotoxicity plus genotoxicity) of MCAcAm ( $1310 \text{ M}^{-1}$ ) was significantly higher than DCAcAm ( $168 \text{ M}^{-1}$ ) and TCaAm ( $233 \text{ M}^{-1}$ ) (Table SM2). To further compare the toxic effect of HACaMs during ZVI reductive dehalogenation, we undertook a preliminary toxic risk analysis by calculating the toxic risk value of each HACaM (Yang et al., 2014), obtained by multiplying the combined toxicity value (Plewa et al., 2008) by its concentration as recorded under different conditions during this study. Then, the integrated toxic risk value was calculated by summing values for the three chlorinated HACaM (Table SM2), as shown in Fig. 1f. The relative calculation formula is shown below:



$$\text{ITRV}_t = \Sigma[\text{CTV}_{\text{HAcAm}} \times \text{C}_{\text{HAcAm}, t}] \quad (8)$$

$\text{ITRV}_t$  — Integrated toxic risk value at  $t$  h

$\text{CTV}_{\text{HAcAm}}$  — Combined toxicity value ( $\text{M}^{-1}$ ) of each detected HAcAm

$\text{C}_{\text{HAcAm}, t}$  — Concentration of each HAcAm (nM) at  $t$  h

As shown in Fig. 1f, at ZVI = 0.2 g/L, the integrated toxic risk value for the three chlorinated HAcAms over 24 h was stable due to low removal of TCACAm. When the ZVI dosage was increased to 5.0 g/L, the integrated toxic risk decreased from the initial value of  $1.20 \times 10^6$  to  $5.76 \times 10^5$  at 6 h, and then increased to  $9.02 \times 10^5$  at 12 h and  $7.75 \times 10^5$  at 24 h. This is mainly attributable to the formation of MCACAm over long time periods (Fig. 1c), as this compound has higher combined toxicity than DCACAm and TCACAm (Plewa et al., 2008; Table SM2). When the ZVI dose was further increased to 10.0 g/L, the pattern of integrated toxic risk values was similar to ZVI = 5.0 g/L, except that values were further decreased to  $3.43 \times 10^5$  at 24 h due to removal of MCACAm at the highest ZVI dose (10.0 g/L). Since MCACAm, which has high combined toxicity, was not effectively removed, the ability of ZVI to dehalogenate HAcAms needs to be enhanced.

### 3.3. Removal of HAcAms by metallic Cu

As shown in Fig. SM3, the concentrations of TCACAm did not change significantly at applied Cu doses, and DCACAm and MCACAm were undetectable over 24 h. As DCACAm and MCACAm were not formed from TCACAm, the effect of Cu alone on reduction of DCACAm and MCACAm was investigated separately. The results showed that Cu alone was also not effective for the reduction of DCACAm and MCACAm. Therefore, it was confirmed that metallic Cu alone cannot effectively reduce the three chlorinated HAcAms in drinking water. This is because Cu(II) ( $E^0_{[\text{Cu}^{2+}/\text{Cu}]} = +0.34$  V at 25 °C) has a significantly higher (more positive) reduction potential than Fe(II) ( $E^0_{[\text{Fe}^{2+}/\text{Fe}]} = -0.45$  V at 25 °C) (Hoang et al., 2011).

### 3.4. Removal of HAcAms by ZVI/Cu

The impact of Cu addition on the reduction of HAcAms by ZVI was also investigated (Fig. SM4). As seen, the dechlorination of TCACAm was increased when Cu and ZVI were dosed together into TCACAm solution. The pseudo-first-order reduction rate of TCACAm increased from  $0.43 \text{ h}^{-1}$  (Table SM1) to  $0.60 \text{ h}^{-1}$  (Table SM3) when ZVI alone was changed to ZVI/Cu at ZVI/Cu molar ratio = 1:1 and pH = 7.0. Fig. SM4 investigated the influence of ZVI/Cu molar ratio on the removal of HAcAms. The reduction in TCACAm reached the optimal efficiency at a ZVI/Cu molar ratio of 1:1.82.3% TCACAm was reduced at ZVI dose = 10.0 g/L after 3 h. After 24 h, TCACAm and DCACAm were both undetectable at all selected ZVI/Cu molar ratios at ZVI dose = 10.0 g/L. Thus, only MCACAm was detected and moreover MCACAm was reduced to below the detection limit when the ZVI/Cu molar ratio was 1:1. In general, the addition of Cu strengthened the reductive dehalogenation of HAcAms by ZVI, and the optimal ZVI/Cu molar ratio was 1:1 for reduction of HAcAms. As previously reported, in the primary battery system, the potential difference between Fe and Cu (0.78 V) is even higher than that between Fe and  $\text{Fe}^{2+}$  (0.45 V), thereby the addition of Cu can accelerate corrosion of the ZVI surface and raise the reactivity of ZVI (Ma and Zhang, 2008; Xiong et al., 2015). However, excess Cu can cover the reaction sites on the surface of ZVI, which negatively impacts reduction (Jiao et al., 2009; Lai et al., 2014). Therefore, ZVI/Cu molar ratio of 1:1 was selected for subsequent tests.

### 3.5. The impact of pH on the removal of chlorinated HAcAms by ZVI/Cu

Fig. 2 shows the effect of solution pH on the dechlorination of TCACAm by ZVI and Cu at a molar ratio of 1:1. As shown in Fig. 2a, TCACAm reduction rates (Table SM3) accelerated from  $0.02 \text{ h}^{-1}$  to  $2.23 \text{ h}^{-1}$  as pH decreased from 8.0 to 5.0, this result being similar to the previous reports (Fang et al., 2011; Xia et al., 2014; Zhang et al., 2006; Jovanovic et al., 2005). At a relatively high pH (e.g., pH = 8.0), a passivation layer (a layer formed by the corrosion products, such as  $\text{Fe}(\text{OH})_2$ ,  $\text{Fe}(\text{OH})_3$ ,  $\text{FeCO}_3$  and so on) can be produced on the surface of ZVI, which can suppress additional dechlorination reaction of TCACAm (Fang et al., 2011; Xia et al., 2014). However, since neither DCACAm (Fig. 2b) nor MCACAm (Fig. 2c) was detected, this indicated the reduction of TCACAm was attributable to the base-catalyzed hydrolysis of HAcAms (Glezer et al., 1999; Chu et al., 2009a). A previous study reported the hydrolysis rate constant of TCACAm at pH = 8.0 was  $0.015 \text{ h}^{-1}$  (Chu et al., 2009a), which was slightly lower than the reduction rate constant ( $0.020 \text{ h}^{-1}$ , Table SM3) recorded for TCACAm at pH = 8.0 in the present study. When the reduction rate constant ( $0.020 \text{ h}^{-1}$ ) was separated from the hydrolysis rate constant ( $0.015 \text{ h}^{-1}$ ), the remained reduction rate constant ( $0.005 \text{ h}^{-1}$ ) was probably attributed to that a small amount of TCACAm was probably dechlorinated by ZVI/Cu at pH = 8.0, the DCACAm formed could be hydrolyzed to DCAA (Glezer et al., 1999; Chu et al., 2009a; Yu and Reckhow, 2015). To confirm this hypothesis, we analyzed the concentrations of three HAAs. At pH = 8.0, as shown in Fig. 2e, the three HAAs were not detected during the initial 1 h, whereas TCAA concentrations at 3, 6, 12 and 24 h were  $0.35 \pm 0.02$ ,  $0.46 \pm 0.02$ ,  $0.54 \pm 0.03$  and  $0.77 \pm 0.04 \mu\text{M}$ , respectively (Fig. 2e). DCAA ( $0.14 \pm 0.01 \mu\text{M}$ ) was also detected at 24 h, which is in agreement with the above-mentioned hypothesis and corresponds with results from previous studies examining the hydrolysis of haloacetonitriles and HAcAms (Chu et al., 2009a; Yu and Reckhow, 2015). MCAA was not detected, indicating dechlorination of neither of TCACAm nor TCAA was significant under these conditions. This is consistent with a previous study which also found that ZVI/Cu may effectively remove HAAs in water at pH 7.0, but was ineffective under alkaline conditions (Chu et al., 2009b).

At lower pH values (e.g., pH = 5.0 and 6.0), all three HAAs were undetected (Fig. 2e). This can be explained by limited hydrolysis of HAcAms to HAAs under acidic conditions (Chu et al., 2013; Yu and Reckhow, 2015). However, the ZVI corrosion (the reduction of ZVI to  $\text{Fe}^{2+}$ ) was accelerated in a weakly acid environment, which can promote dechlorination of TCACAm by Equation (2) (Noubactep, 2008; Zhang et al., 2006; Jovanovic et al., 2005). At pH 5.0 and pH 6.0, the concentrations of DCACAm initially increased to  $1.31 \pm 0.07 \mu\text{M}$  and  $1.49 \pm 0.07 \mu\text{M}$  respectively at 1 h, and then rapidly decreased to below the detection limit at 3 h (Fig. 2b). Unlike DCACAm, the concentrations of MCACAm initially increased to  $3.57 \pm 0.18 \mu\text{M}$  and  $2.17 \pm 0.11 \mu\text{M}$  after 3 h at pH 5.0 and pH 6.0, respectively, and then slowly decreased to  $2.44 \pm 0.12 \mu\text{M}$  and  $1.14 \pm 0.06 \mu\text{M}$  at 24 h, respectively (Fig. 2c). Of note, the reduction of MCACAm at pH 5.0 and pH 6.0 was less than at pH 7.0, which also resulted in poorer removal for the sum of three HAcAms at pH 5.0 and pH 6.0 than pH 7.0 at 24 h (Fig. 2d). As discussed in Section 3.1, limited Fe oxide was formed on ZVI at pH 7.0, which potentially adsorbed a fraction of the MCACAm formed.

As shown in Fig. 2f, we also compared the integrated toxic risk values of HAcAms at different pHs (Table SM4). Although TCACAm and DCACAm were removed effectively at pH 5.0 and pH 6.0, the integrated toxic risk values ( $3.79 \times 10^6$  and  $2.26 \times 10^6$  at 12 h) for the HAcAms were relatively higher than at pH = 7.0 ( $1.13 \times 10^6$  at 12 h), due to the poor removal of MCACAm. Additionally, integrated toxic risk values for HAcAms at pH = 8.0 ( $9.76 \times 10^5$  at 12 h) were

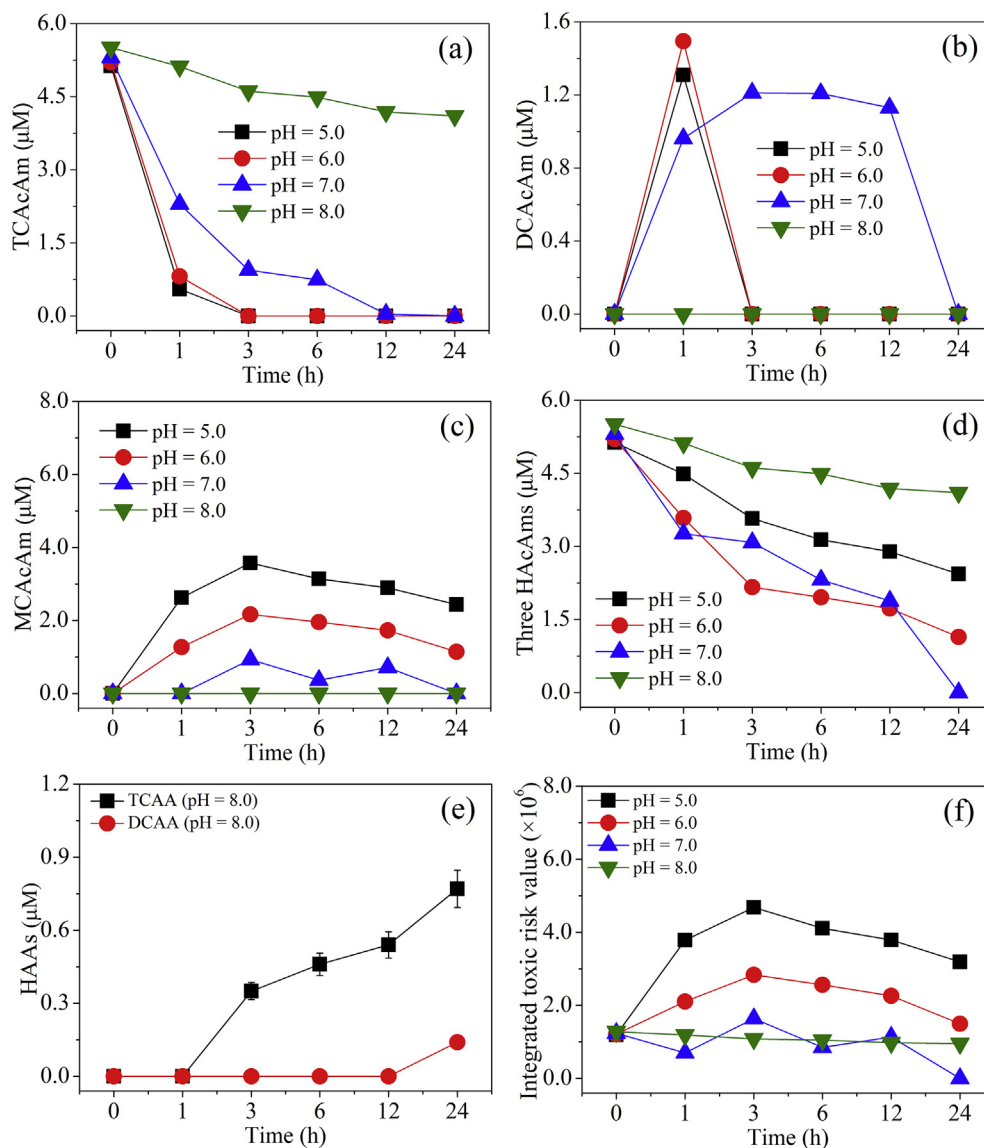


**Fig. 2.** Influence of pH on the removal of HACams by ZVI/Cu. (Initial TCACAm molar concentration =  $5.30 \mu\text{M}$  [DCACAm and MCACAm were not added]. ZVI dosage =  $10.0 \text{ g/L}$  [ZVI/Cu molar ratio = 1:1]).

similar to at pH = 7.0 ( $1.13 \times 10^6$  at 12 h) before 12 h, mainly because MCACAm with higher combined toxicity was not formed from the dechlorination of TCACAm by ZVI/Cu at pH = 8.0. In general, the neutral condition was most conducive to the total removal of TCACAm, DCACAm and MCACAm by ZVI/Cu.

### 3.6. The impact of temperature on the removal of HACams by ZVI/Cu

As shown in Fig. 3, reduction of TCACAm increased as the temperature increased from  $10^\circ\text{C}$  to  $40^\circ\text{C}$ . We calculated the activation energies ( $E_a$ ) for the reaction between ZVI/Cu and TCACAm using the Arrhenius plot (Arrhenius, 1889) and the pseudo first order reaction rate constants at different temperatures (Fig. SM5). The  $E_a$  in the reaction between ZVI/Cu and TCACAm is  $52.8 \text{ kJ/mol}$ . This is lower than that for many common chemical reactions ( $60\text{--}250 \text{ kJ/mol}$ ) (Laidler, 1993), which indicates the reaction is expected to proceed under ambient conditions. At  $40^\circ\text{C}$ , TCACAm was removed completely inside 3 h. DCACAm and MCACAm were both detected at 1 h, but were also both reduced to below the detection limits inside

3 h (see Fig. SM6). At  $10^\circ\text{C}$ , the reduction rates of three HACams were relatively slower than at  $25^\circ\text{C}$ . The concentrations of DCACAm initially increased to  $1.44 \pm 0.07 \mu\text{M}$  at 3 h, and then rapidly decreased to  $0.98 \pm 0.05 \mu\text{M}$  at 24 h. Further, concentrations of MCACAm continuously increased over 24 h (from  $0.30 \pm 0.02 \mu\text{M}$  at 3 h to  $1.14 \pm 0.06 \mu\text{M}$  at 24 h). This also resulted in high integrated toxic risk value ( $1.71 \times 10^6$ ) from the HACams at 24 h and  $10^\circ\text{C}$  (Fig. SM7 and Table SM5).

### 3.7. Removal of brominated HACams by ZVI/Cu

The dehalogenation of BDCACAm, DBCACAm and TBACAm by ZVI/Cu was investigated at  $\text{pH } 6.0 \pm 0.2$  to avoid the effect of hydrolysis of HACams (Chu et al., 2009a, 2013; Yu and Reckhow, 2015). The removal of three brominated HACams by ZVI at pH 6.0 was also investigated, and the removal and formation trend of HACams was in agreement with that by ZVI/Cu. However, the removal efficiency of HACAm by ZVI was significantly inferior to ZVI/Cu (Fig. SM8). As shown in Fig. 4a and b, DCACAm and BCACAm were firstly formed from the debromination of BDCACAm and

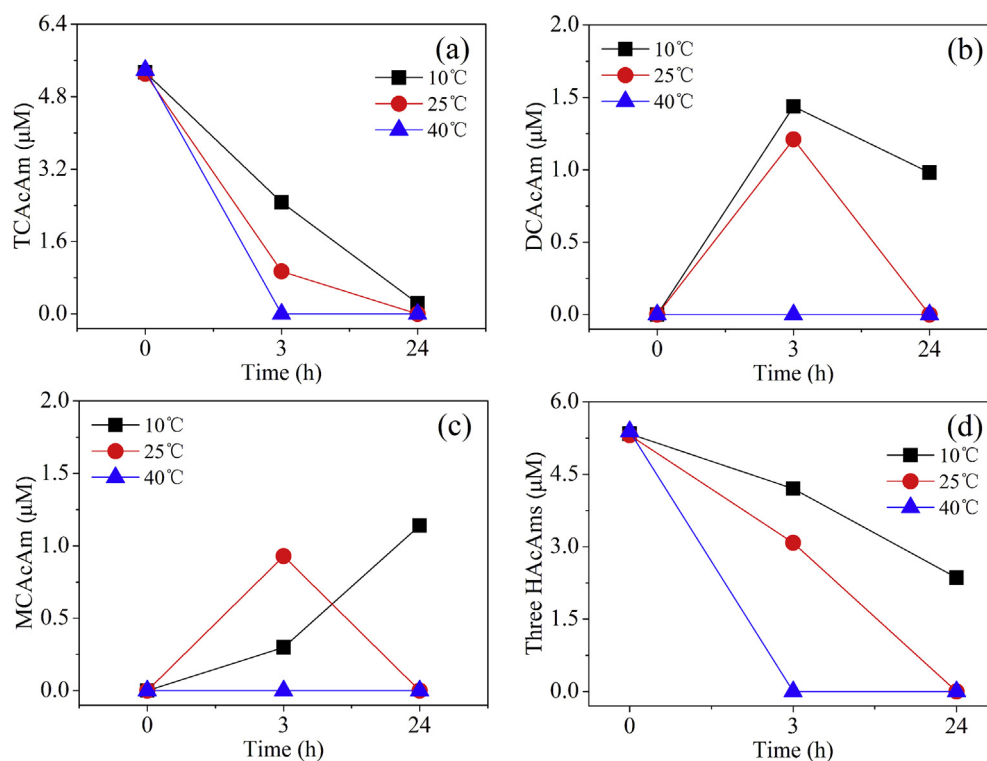


**Fig. 3.** Influence of temperature on the removal of HACams by ZVI/Cu. (Initial TCACAm molar concentration = 5.30 μM [DCACAm and MCACAm were not added]. ZVI dosage = 10.0 g/L [ZVI/Cu molar ratio = 1:1]).

BDCACAm, respectively. Subsequently, DCACAm and BCACAm concentrations were further decreased, and only MCACAm was recorded from the dechlorination and debromination of DCACAm and BCACAm, respectively. This result directly suggests that bromine was preferentially removed over chlorine in HACams by ZVI/Cu.

Because of this, BDCACAm, DBCACAm and TBACAm concentrations were all rapidly reduced to a very low level (near the detection limit) inside 1 h (Fig. 4a, b and c), and the removal rates (98.7%, 97.6% and 96.4%) of three brominated HACams were all higher than for TCACAm (84.3%) under the same reaction conditions (Fig. SM9). Additionally, as shown in Fig. 4c, only MBACAm was observed from 3 h to 24 h, and only MCACAm was left from 3 h to 24 h for BDCACAm (Fig. 4a), DBCACAm (Fig. 4b) and TCACAm (Fig. 4d) at pH 6.0. Therefore, a plot of the pseudo-first-order reduction rate of MCACAm (from dehalogenation of TCACAm, BDCACAm and DBCACAm) and MBACAm (from TBACAm) from 3 h to 24 h is presented in Fig. 4e. The reduction rate for MBACAm ( $k_{\text{obs}} = 0.079 \text{ h}^{-1}$ ) was comparatively higher than for MCACAm ( $k_{\text{obs}} = 0.030, 0.036 \text{ and } 0.037 \text{ h}^{-1}$ ). These results all indicated that brominated HACams were more easily reduced than chlorinated HACams by ZVI/Cu, which is in agreement with a previous study examining the removal of HAAs by ZVI (Hozalski et al., 2001). Although the electronegativity of chlorine (3.16) is greater than bromine (2.96), the bond length of the C–Br bond ( $194 \times 10^{-12} \text{ m}$ ) is higher than the C–Cl bond ( $177 \times 10^{-12} \text{ m}$ ) (Haynes, 2013; Linus, 1932), which equates to the former being weaker than the latter (March 1992).

Fig. 4f compares the integrated toxic risk from TCACAm, BDCACAm, DBCACAm, and TBACAm during ZVI/Cu reduction. After 3 h, the integrated toxic risk from reduced solutions of TCACAm, BDCACAm and DBCACAm all decreased, whereas the integrated toxic risk from TBACAm was higher from 3 h ( $6.58 \times 10^7$ ) to 24 h ( $1.23 \times 10^7$ ), because only TBACAm, which has high combined

toxicity (Table SM6), formed MBACAm during ZVI/Cu dehalogenation reduction under these conditions. Therefore, reduction of TBACAm caused a higher toxicity risk than reductions of TCACAm, even though TBACAm was more easily dehalogenated than TCACAm by ZVI/Cu dehalogenation.

#### 4. Conclusions

ZVI alone can dechlorinate TCACAm to sequentially form DCACAm and MCACAm. The strong correlation between the theoretical calculated  $\text{Fe}^{2+}$  concentrations and the actual detected  $\text{Fe}^{2+}$  concentrations release suggests the reduction of TCACAm is mainly attributable to direct dechlorination of TCACAm by ZVI. At increased ZVI doses, the reduction rate of TCACAm was accelerated, and the integrated toxic risks caused by total concentrations of TCACAm, DCACAm and MCACAm decreased.

Metallic Cu alone did not affect HACAm concentrations, but the addition of Cu to ZVI significantly improved the removal of HACams during ZVI dehalogenation. TCACAm and its reduction products (DCACAm and MCACAm) were all decreased to under detection limits at a ZVI/Cu molar ratio of 1:1 and 24 h.

Dechlorination of TCACAm by ZVI/Cu increased with the decreasing pH from 8.0 to 5.0. The slight decrease in TCACAm concentration at pH = 8.0 was explained by base-catalyzed hydrolysis of HACams, rather than dechlorination of TCACAm by ZVI/Cu. Under acidic conditions TCACAm dechlorination reaction was promoted, while the integrated toxic risk was minimised at pH 7.0, due to poor removal of the reduction product MCACAm at pH = 5.0 and 6.0. Additionally, the reductive dehalogenation of HACams had a low  $E_a$  value, and was increased at the temperature increased from 10 °C to 25 °C–40 °C. The lower temperature resulted in higher integrated toxic risk value due to the increased formation of MCACAm.

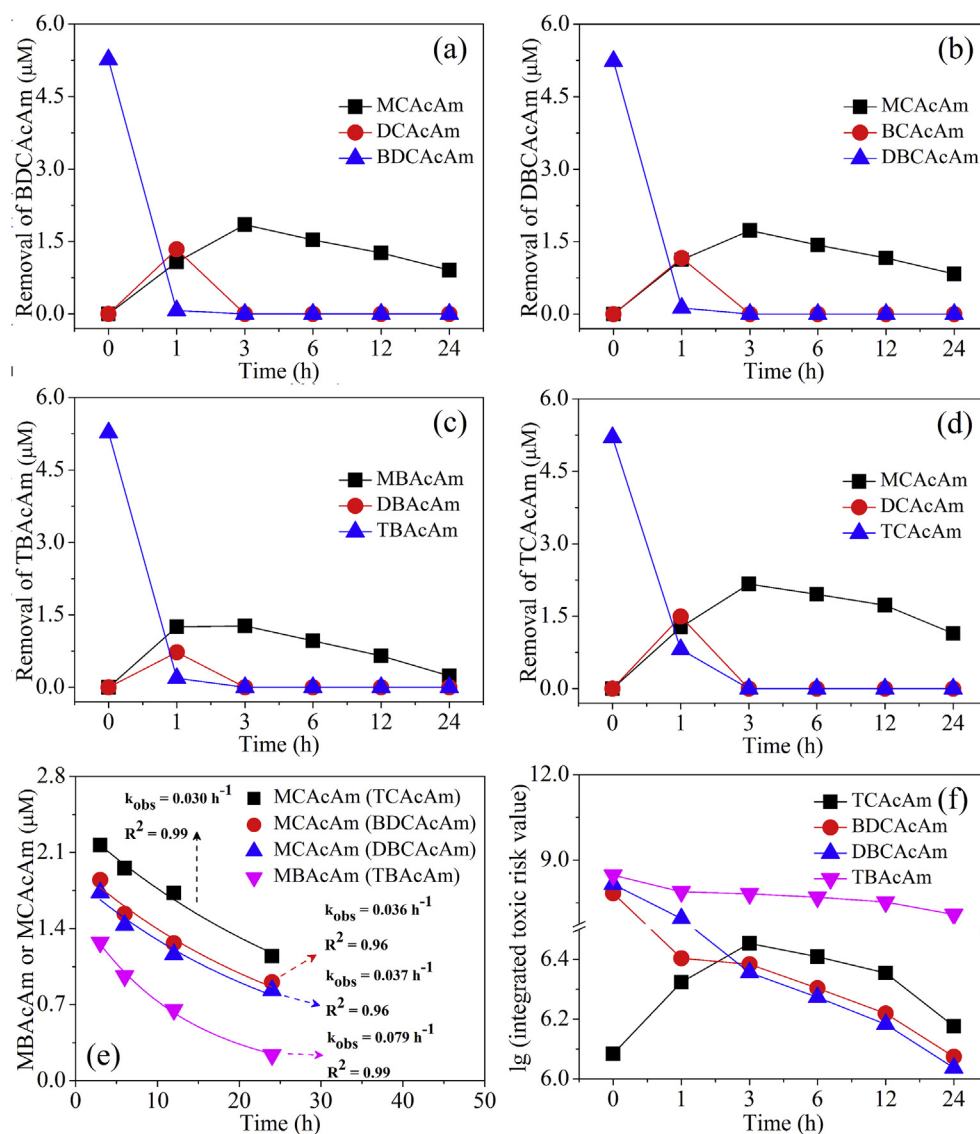


**Fig. 4.** Removal of brominated HACams by ZVI/Cu at pH 6.0. (Initial tri-brominated HACAm molar concentration = 5.30  $\mu\text{M}$  [BDCAcAm, DBCAcAm and TBACAm were added for Fig. 4a–c]; ZVI dosage = 10.0 g/L [ZVI/Cu molar ratio = 1:1]; a, BDCAcAm removal; b, DBCAcAm removal; c, TBACAm removal; d, removal rate (%) of four tri-HACams at 1 h by ZVI/Cu; e, the pseudo-first-order reduction rate of MCAcAm [Fig. 4a and b] and MBACAm [Fig. 4c] from 3 h to 24 h; f, integrated toxic risk caused by HACams at pH 6.0.).

Bromine was preferentially removed over chlorine in HACams during ZVI/Cu dehalogenation, as higher overall removal of brominated HACams than chlorinated HACams was recorded. However, TBACAm caused higher integrated toxicity risk than TCACAm, even though TBACAm was more easily removed than TCACAm during ZVI/Cu reduction, due to the formation of MBACAm during debromination of TBACAm.

In distribution systems, any ZVI present in the passive layer of cast iron pipes will come into contact with treated water. This highlights the potential for the formation of monohaloacetamides (MCAcAm and MBACAm), with higher toxicity than trihaloacetamides and dihaloacetamides, from ZVI-mediated reactions during drinking water distribution. This study demonstrates that higher ZVI/Cu exposure - 10 g/L ZVI and 11 g/L Cu - effectively reduces the integrated toxicity risks (based on combined cytotoxicity and genotoxicity) at neutral conditions and ambient temperatures. However, investigations at pilot- and/or full-scale are required to fully understand the magnitude of reductive dehalogenation which occurs in real-life distribution systems.

## Acknowledgements

The authors gratefully acknowledge the National Major Science and Technology Project of China (No. 2015ZX07406-004-03).

## Appendix A. Supplementary data

Supplementary data related to this article can be found at <http://dx.doi.org/10.1016/j.watres.2016.10.047>.

## References

- Arrhenius, S.A., 1889. Über die Dissociationswärme und den Einfluss der Temperatur auf den Dissoziationsgrad der Elektrolyte. *Z. Phys. Chem.* 4, 96–116.
- Bond, T., Huang, J., Templeton, M.R., Graham, N., 2011. Occurrence and control of nitrogenous disinfection by-products in drinking water - a review. *Water Res.* 45 (15), 4341–4354.
- Bond, T., Templeton, M.R., Mokhtar, K., Nurul, H., Graham, N., Kanda, R., 2015. Nitrogenous disinfection byproducts in English drinking water supply systems: occurrence, bromine substitution and correlation analysis. *Water Res.* 85, 85–94.



- Chu, W.H., Gao, N.Y., Deng, Y., 2009a. Stability of new found nitrogenous disinfection by-products: haloacetamides in drinking water. *Chin. J. Org. Chem.* 29 (10), 1569–1574.
- Chu, W.H., Gao, N.Y., Zhao, S.J., Dong, B.Z., 2009b. Removal of halogenated disinfection by-products trichloroacetic acid by Fe/Cu catalytic reduction in drinking water. *J. Tongji Univ. Nat. Sci.* 37 (10), 1355–1359.
- Chu, W.H., Gao, N.Y., Deng, Y., Templeton, M.R., Yin, D.Q., 2011. Impacts of drinking water pretreatments on the formation of nitrogenous disinfection by-products. *Bioresour. Technol.* 102 (24), 11161–11166.
- Chu, W.H., Gao, N.Y., Yin, D.Q., Krasner, S.W., Templeton, M.R., 2012. Trace determination of 13 haloacetamides in drinking water using liquid chromatography triple quadrupole mass spectrometry with atmospheric pressure chemical ionization. *J. Chromatogr. A* 1235, 178–181.
- Chu, W.H., Gao, N.Y., Yin, D.Q., Krasner, S.W., 2013. Formation and speciation of nine haloacetamides, an emerging class of nitrogenous DBPs, during chlorination or chloramination. *J. Hazard. Mater.* 260, 806–812.
- Chu, W.H., Gao, N.Y., Yin, D.Q., et al., 2014. Impact of UV/H<sub>2</sub>O<sub>2</sub> pre-oxidation on the formation of haloacetamides and other nitrogenous disinfection byproducts during chlorination. *Environ. Sci. Technol.* 48 (20), 12190–12198.
- Chu, W.H., Li, D.M., Gao, N.Y., et al., 2015a. The control of emerging haloacetamide DBP precursors with UV/persulfate treatment. *Water Res.* 72, 340–348.
- Chu, W.H., Li, X., Gao, N.Y., et al., 2015b. Peptide bonds affect the formation of haloacetamides, an emerging class of N-DBPs in drinking water: free amino acids versus oligopeptides. *Sci. Rep.* 5, 14412.
- Critchley, M.M., Cromar, N.J., McClure, N., Fallowfield, H.J., 2001. Biofilms and microbially influenced cuprosolvency in domestic copper plumbing systems. *J. Appl. Microbiol.* 91, 646–651.
- Cwierny, D.M., Bransfield, S.J., Livi, K.J.T., Fairbrother, D.H., Roberts, A.L., 2006. Exploring the influence of granular iron additives on 1,1,1-trichloroethane reduction. *Environ. Sci. Technol.* 40 (21), 6837–6843.
- Dotson, A., Westerhoff, P., 2009. Occurrence and removal of amino acids during drinking water treatment. *J. Am. Water Works Assoc.* 101 (9), 101–115.
- Dries, J., Bastiaens, L., Springael, D., Agathos, S.N., Diels, L., 2004. Competition for sorption and degradation of chlorinated ethenes in batch zero-valent iron systems. *Environ. Sci. Technol.* 38 (10), 2879–2884.
- Fang, Z.Q., Chen, J.H., Qiu, X.H., Qiu, X.Q., Cheng, W., Zhu, L.C., 2011. Effective removal of antibiotic metronidazole from water by nanoscale zero-valent iron particles. *Desalination* 268, 60–67.
- Feng, J., Lim, T.T., 2007. Iron-mediated reduction rates and pathways of halogenated methanes with nanoscale Pd/Fe: analysis of linear free energy relationship. *Chemosphere* 66 (9), 1765–1774.
- Gillham, R.W., O'Hannesin, S.F., 1994. Enhanced degradation of halogenated aliphatics by zero-valent iron. *Ground Water* 32 (6), 958–967.
- Glezer, V., Harris, B., Tal, N., Josefzon, B., Lev, O., 1999. Hydrolysis of haloacetonitriles: linear free energy relationship, kinetics and products. *Water Res.* 33, 1938–1948.
- Goslan, E.H., Krasner, S.W., Bower, M., Rocks, S.A., Holmes, P., Levy, L.S., Parsons, S.A., 2009. A comparison of disinfection by-products found in chlorinated and chloraminated drinking waters in Scotland. *Water Res.* 43 (18), 4698–4706.
- Guan, X.H., Sun, Y.K., Qin, H.J., Li, J.X., Lo, I.M.C., He, D., Dong, H.R., 2015. The limitations of applying zero-valent iron technology in contaminants sequestration and the corresponding countermeasures: the development in zero-valent iron technology in the last two decades (1994–2014). *Water Res.* 75, 224–248.
- He, F., Zhao, D.Y., Paul, C., 2010. Field assessment of carboxymethyl cellulose stabilized iron nanoparticles for in situ destruction of chlorinated solvents in source zones. *Water Res.* 44, 2360–2370.
- Haynes, W.M., 2013. *CRC Handbook of Chemistry and Physics*, 94th ed. CRC Press, Boca Raton, FL.
- Hoang, D.L., Dang, T.H., Engeldinger, J., Schneider, M., Radnik, J., Richter, M., Martin, A., 2011. TPR investigations on the reducibility of Cu supported on Al<sub>2</sub>O<sub>3</sub>, zeolite Y and SAPO-5. *J. Solid State Chem.* 184, 1915–1923.
- Hou, Y.K., Chu, W.H., Ma, M., 2012. Carbonaceous and nitrogenous disinfection by-product formation in the surface and ground water treatment plants using Yellow River as water source. *J. Environ. Sci.* 24 (7), 1204–1209.
- House, H.O., 1972. *Modern Synthetic Reactions*, second ed. Benjamin, Menlo Park, CA, pp. 145–227.
- Hozalski, R.M., Li, Z., Arnold, W.A., 2001. Reduction of haloacetic acids by Fe<sup>0</sup>: implications for treatment and fate. *Environ. Sci. Technol.* 35, 2258–2263.
- Huang, H., Wu, Q.Y., Hu, H.Y., Mitch, W.A., 2012. Dichloroacetonitrile and dichloroacetamide can form independently during chlorination and chloramination of drinking waters, model organic matters, and wastewater effluents. *Environ. Sci. Technol.* 46 (19), 10624–10631.
- Jiao, Y.L., Qiu, C.C., Huang, L.H., Wu, K.X., Ma, H.Y., Chen, S.H., Ma, L.M., Wu, D.L., 2009. Reductive dechlorination of carbon tetrachloride by zero-valent iron and related iron corrosion. *Appl. Catal. B Environ.* 91 (1–2), 434–440.
- Jovanovic, G.N., Znidarsic-Plazl, P., Sakrithichai, P., Al-Khaldi, K., 2005. Dechlorination of p-chlorophenol in a microreactor with bimetallic Pd/Fe catalyst. *Ind. Eng. Chem. Res.* 44, 5099–5106.
- Keenan, C.R., Sedlak, D.L., 2008. Factors affecting the yield of oxidants from the reaction of manoparticulate zero-valent iron and oxygen. *Environ. Sci. Technol.* 42 (4), 1262–1267.
- Kohn, T., Livi, K.J.T., Roberts, A.L., Vikesland, P.J., 2005. Longevity of granular iron in groundwater treatment processes: corrosion product development. *Environ. Sci. Technol.* 39 (8), 2867–2879.
- Kooij, D.v.d., Veenendaal, H.R., Scheffer, W.J.H., 2005. Biofilm formation and multiplication of *Legionella* in a model warm water system with pipes of copper, stainless steel and cross-linked polyethylene. *Water Res.* 39 (13), 2789–2798.
- Krasner, S.W., Mitch, W.A., McCurry, D.L., Hanigan, D., Westerhoff, P., 2013. Formation, precursors, control, and occurrence of nitrosamines in drinking water: a review. *Water Res.* 47 (13), 4433–4450.
- Krasner, S.W., Weinberg, H.S., Richardson, S.D., Pastor, S.J., Chinn, R., Scimanti, M.J., Onstad, G.D., Thruston, A.D., 2006. Occurrence of a new generation of disinfection byproducts. *Environ. Sci. Technol.* 40 (23), 7175–7185.
- Lai, B., Zhang, Y.H., Chen, Z.Y., Yang, P., Zhou, Y.X., Wang, J.L., 2014. Removal of p-nitrophenol (PNP) in aqueous solution by the micro-scale iron-copper (Fe/Cu) bimetallic particles. *Appl. Catal. B Environ.* 144, 816–830.
- Laidler, K.J., 1993. *The World of Physical Chemistry*. Oxford University Press, Oxford.
- Lehtola, M.J., Miettinen, I.T., Keinänen, M.M., Kekki, T.K., Laine, O., Hirvonen, A., Vartiainen, T., Martikainen, P.J., 2004. Microbiology, chemistry and biofilm development in a pilot drinking water distribution system with copper and plastic pipes. *Water Res.* 38 (17), 3769–3779.
- Liang, L.P., Guan, X.H., Shi, Z., Li, J.L., Wu, Y.N., Paul, G.T., 2014. Coupled effects of aging and weak magnetic fields on sequestration of selenite by zero-valent iron. *Environ. Sci. Technol.* 48 (11), 6326–6334.
- Lien, H.L., Zhang, W.X., 2001. Nanoscale iron particles for complete reduction of chlorinated ethenes. *Colloids Surf., A Physicochem. Eng. Aspects* 191 (1–2), 97–105.
- Lien, H.L., Zhang, W.X., 2005. Hydrodechlorination of chlorinated ethanes by nanoscale Pd/Fe bimetallic particles. *J. Environ. Eng.* 131 (1), 4–10.
- Lin, J.P., Ellaway, M., Adrien, R., 2001. Study of corrosion material accumulated on the inner wall of steel water pipe. *Corros. Sci.* 43 (11), 2065–2081.
- Linus, P., 1932. The nature of the chemical bond. iv. The energy of single bonds and the relative electronegativity of atoms. *J. Am. Chem. Soc.* 54 (9), 3570–3582.
- Liu, Y.Q., Lowry, G.V., 2006. Effect of particle age (Fe<sup>0</sup> content) and solution pH on NZVI reactivity: H<sub>2</sub> evolution and TCE dechlorination. *Environ. Sci. Technol.* 40 (19), 6085–6090.
- Liu, J., Zhang, X.R., 2014. Comparative toxicity of new halophenolic DBPs in chlorinated saline wastewater effluents against a marine alga: halophenolic DBPs are generally more toxic than haloaliphatic ones. *Water Res.* 65, 64–72.
- Liu, X., Zhang, Y., Han, W., Tang, A., Shen, J., Cui, Z., Vitousek, P., Erisman, J.W., Goulding, K., Christie, P., Fangmeier, A., Zhang, F., 2013. Enhanced nitrogen deposition over China. *Nature* 494 (7438), 459–462.
- Ma, L.M., Zhang, W.X., 2008. Enhanced biological treatment of industrial wastewater with bimetallic zero-valent iron. *Environ. Sci. Technol.* 42 (15), 5384–5389.
- Maithreepala, R.A., Doong, R.A., 2004. Reductive dechlorination of carbon tetrachloride in aqueous solutions containing ferrous and copper ions. *Environ. Sci. Technol.* 38 (24), 6676–6684.
- March, J., 1992. *Advanced Organic Chemistry*. Wiley-Interscience, New York.
- McNeill, L.S., Edwards, M., 2001. Iron pipe corrosion in distribution systems. *J. Am. Water Works Ass.* 93 (7), 88–101.
- Niquette, P., Servais, P., Savoir, R., 2000. Impacts of pipe materials on densities of fixed bacterial biomass in a drinking water distribution system. *Water Res.* 34 (6), 1952–1956.
- Noubactep, C., 2008. A critical review on the process of contaminant removal in Fe<sup>0</sup>-H<sub>2</sub>O systems. *Environ. Sci. Technol.* 29 (8), 909–920.
- Plewa, M.J., Muellner, M.G., Richardson, S.D., Fasano, F., Buettner, K.M., Woo, Y.T., McKague, A.B., Wagner, E.D., 2008. Occurrence, synthesis, and mammalian cell cytotoxicity and genotoxicity of haloacetamides: an emerging class of nitrogenous drinking water disinfection byproducts. *Environ. Sci. Technol.* 42 (3), 955–961.
- Plewa, M.J., Wanger, E.D., 2015. Charting a new path to resolve the adverse health effects of DBPs. In: Karanfil, Tanju, Mitch, Bill, Westerhoff, Paul, Xie, Yuefeng (Eds.), *Recent Advances in Disinfection By-products*. American Chemical Society, Washington, DC, pp. 3–23 (Chapter 1).
- Plewa, M.J., Wagner, E.D., Muellner, M.G., Hsu, K.M., Richardson, S.D., 2007. Comparative mammalian cell toxicity of N-DBPs and C-DBPs. In: ACS Symposium Series. Oxford University Press.
- Reckhow, D.A., Platt, T.L., MacNeill, A.L., McClellan, J.N., 2001. Formation and degradation of dichloroacetonitrile in drinking waters. *J. Water Supply Res. Technol. Aqua* 50 (1), 1–13.
- Richardson, S.D., Plewa, M.J., Wagner, E.D., Schoeny, R., DeMarini, D.M., 2007. Occurrence, genotoxicity, and carcinogenicity of regulated and emerging disinfection by-products in drinking water: a review and roadmap for research. *Mutat. Res.* 636 (1–3), 178–242.
- Richardson, S.D., Postigo, C., 2015. Formation of DBPs: state of the science. In: Karanfil, Tanju, Mitch, Bill, Westerhoff, Paul, Xie, Yuefeng (Eds.), *Recent Advances in Disinfection By-products*. American Chemical Society, Washington, DC, pp. 189–214 (Chapter 11).
- Richardson, S.D., Ternes, T.A., 2014. Water analysis: emerging contaminants and current issues. *Anal. Chem.* 86 (6), 2813–2848.
- Richardson, S.D., Thruston Jr., A.D., Krasner, S.W., Weinberg, H.S., Miltner, R.J., Schenck, K.M., Narotsky, M.G., McKague, A.B., Simmons, J.E., 2008. Integrated disinfection by-products mixtures research: comprehensive characterization of water concentrates prepared from chlorinated and ozonated/postchlorinated drinking water. *J. Toxicol. Environ. Health Pt. A* 71 (17), 1165–1186.
- Ridgway, H.F., Means, E.G., Olson, B.H., 1981. Iron bacteria in drinking-water distribution systems: elemental analysis of *Gallionella* stalks, using X-ray energy-dispersive microanalysis. *Appl. Environ. Microb.* 41 (1), 288–297.
- Rossman, L.A., Brown, R.A., Singer, P.C., Nuckols, J.R., 2001. DBP formation kinetics in

- a simulated distribution system. *Water Res.* 35 (14), 3483–3489.
- Shah, A.D., Krasner, S.W., Lee, C.F.T., von Gunten, U., Mitch, W.A., 2012. Trade-offs in disinfection byproduct formation associated with precursor preoxidation for control of N-Nitrosodimethylamine formation. *Environ. Sci. Technol.* 46 (9), 4809–4818.
- Shah, A.D., Mitch, W.A., 2012. Halonitroalkanes, halonitriles, haloamides, and N-nitrosamines: a critical review of nitrogenous disinfection byproduct formation pathways. *Environ. Sci. Technol.* 46 (1), 119–131.
- Tee, Y.H., Bachas, L., Bhattacharyya, D., 2009. Degradation of trichloroethylene by iron-based bimetallic nanoparticles. *J. Phys. Chem. C* 113 (28), 12616–12616.
- Teng, F., Guan, Y.T., Zhu, W.P., 2008. Effect of biofilm on cast iron pipe corrosion in drinking water distribution system: corrosion scales characterization and microbial community structure investigation. *Corros. Sci.* 50 (10), 2816–2823.
- US EPA, 1995. Method 552.2: Determination of Haloacetic Acids and Dalapon in Drinking Water by Liquid–liquid Extraction, Derivatization and Gas Chromatography with Electron Capture Detection. Environmental Monitoring and System Laboratory, Cincinnati, OH.
- Wang, C.B., Zhang, W.X., 1997. Synthesizing nanoscale iron particles for rapid and complete dechlorination of TCE and PCBs. *Environ. Sci. Technol.* 31, 2154–2156.
- Wang, X.Y., Chen, C., Chang, Y., Liu, H.L., 2009. Dechlorination of chlorinated methanes by Pd/Fe bimetallic nanoparticles. *J. Hazard. Mater.* 161 (2–3), 815–823.
- Wang, Y., Le, R.J., Zhang, T., Croué, J.P., 2014. Formation of brominated disinfection byproducts from natural organic matter isolates and model compounds in a sulfate radical-based oxidation process. *Environ. Sci. Technol.* 48 (24), 14534–14542.
- Warren, K.D., Arnold, R.G., Bishop, T.L., Lindholm, L.C., Betterton, E.A., 1995. Kinetics and mechanism of reductive dehalogenation of carbon tetrachloride using zero-valence metals. *J. Hazard. Mater.* 41 (2–3), 217–227.
- Xia, S.Q., Gu, Z.L., Zhang, Z.Q., Zhang, J., Slawomir, W.H., 2014. Removal of chloramphenicol from aqueous solution by nanoscale zero-valent iron particles. *Chem. Eng. J.* 257, 98–104.
- Xie, P.C., Ma, J., Fang, J.Y., Guan, Y.H., Yue, S.Y., Li, X.C., Chen, L.W., 2013. Comparison of permanganate preoxidation and preozonation on algae containing water: cell integrity, characteristics, and chlorinated disinfection byproduct formation. *Environ. Sci. Technol.* 47 (24), 14051–14061.
- Xiong, Z., Lai, B., Yang, P., Zhou, Y., Wang, J., Fang, S., 2015. Comparative study on the reactivity of Fe/Cu bimetallic particles and zero valent iron (ZVI) under different conditions of N<sub>2</sub>, air or without aeration. *J. Hazard. Mater.* 297, 261–268.
- Yang, F., Zhang, J., Chu, W.H., Yin, D.Q., Templeton, M.R., 2014. Haloacetamides versus halomethanes formation and toxicity in chloraminated drinking water. *J. Hazard. Mater.* 274, 156–163.
- Yang, M.T., Zhang, X.R., 2013. Comparative developmental toxicity of new aromatic halogenated DBPs in a chlorinated saline sewage effluent to the marine polychaete *platynereis dumerilii*. *Environ. Sci. Technol.* 47 (19), 10868–10876.
- Yu, Y., Reckhow, D.A., 2015. Kinetic analysis of haloacetonitrile stability in drinking waters. *Environ. Sci. Technol.* 49 (18), 11028–11036.
- Yu, S.L., Lin, T., Chen, W., Tao, H., 2015. The toxicity of a new disinfection by-product, 2,2-dichloroacetamide (DCAcAm), on adult zebrafish (*Danio rerio*) and its occurrence in the chlorinated drinking water. *Chemosphere* 139, 40–46.
- Zhang, W.H., Quan, X., Wang, J.X., Zhang, Z.Y., Chen, S., 2006. Rapid and complete dechlorination of PCP in aqueous solution using Ni-Fe nanoparticles under assistance of ultrasound. *Chemosphere* 65, 58–64.
- Zhang, W.X., Wang, C.B., Lien, H.L., 1998. Treatment of chlorinated organic contaminants with nanoscale bimetallic particles. *Catal. Today* 40 (4), 387–395.
- Zhang, X.L., Deng, B.L., Guo, J., Wang, Y., Lan, Y.Q., 2011. Ligand-assisted degradation of carbon tetrachloride by microscale zero-valent iron. *J. Environ. Manag.* 92 (4), 1328–1333.
- Zhang, Y., Zhang, Z.Y., Zhao, Y.P., Cheng, S.P., Ren, H.Q., 2013. Identifying health effects of exposure to trichloroacetamide using transcriptomics and metabolomics in mice (*Mus musculus*). *Environ. Sci. Technol.* 47 (6), 2918–2924.